

Corrosion Inhibition of Steel in Hydrochloric Acid Solution by New *N,N'*-Bipyrazole Piperazine Derivatives

M. Bouklah¹, M. Kaddouri¹, Y. Toubi¹, B. Hammouti¹, S. Radi¹, E. E. Ebenso^{2,*}

¹LCAE-URAC18, Chemistry Department, Sciences Faculty, University Mohamed Premier, Oujda, Morocco

²Material Science Innovation & Modelling (MaSIM) Focus Area, Faculty of Agriculture, Science and Technology, North-West University (Mafikeng Campus), Private Bag X2046, Mmabatho 2735, South Africa

*E-mail: Eno.Ebenso@nwu.ac.za

Received: 4 March 2013 / Accepted: 14 April 2013 / Published: 1 May 2013

The corrosion inhibition of mild steel in 1M hydrochloric acid solutions by some new *N,N'*-bipyrazole piperazine derivatives namely piperazine (P1), *N,N'*-bis[(3,5-dimethyl-1H-pyrazol-1-yl)methyl]piperazine (P2) and *N,N'*-bis[(3-ethylcarboxylate-5-methyl-1H-pyrazol-1-yl)methyl]piperazine (P3) was studied using chemical (weight loss) and electrochemical (potentiodynamic and electrochemical impedance spectroscopy, EIS) measurements. These measurements show that the inhibition efficiency obtained by these compounds increased by increasing their concentration to attain 91% for P2 and 92% for P3 since 10^{-3} M. The inhibition efficiency follow the order $P3 > P2 > P1$. The inhibition efficiency of (P1 and P2) increases with the rise in temperature in the range 298-353K. Polarization studies show that these compounds act as mixed type inhibitors in 1M HCl solutions. These inhibitors function through adsorption following Langmuir isotherm.

Keywords: Steel, Bipyrazole, Piperazine, Inhibition, Corrosion, Acid.

1. INTRODUCTION

Chemical cleaning and pickling processes are widely used in industrial processes to remove corrosion scales from metallic surface in high concentrated acidic media at elevated temperature between 60 and 95°C [1-2]. Inhibitors are quietly required to protect metals against acid attack. Organic compounds containing electronegative functional groups and π -electron in triple or conjugated double bonds are usually goods inhibitors. Heteroatoms as sulphur, phosphorus, nitrogen and oxygen as well as aromatic ring in their structure are the major adsorption centres.

Recently more study shows that the inhibitive effect found to enhance of several nitrogen containing organic compounds for steel in acid solutions. Organic nitrogen compounds specify of the corrosion behaviour of iron and steel in acidic solutions are usually employed for their rapid action. The synthesis of new pyrazolic, bipyrazolic and tripyrazole compounds is an easy way to obtain several compounds of which the molecular structures contain several heteroatoms and several substituents. This allowed various molecules to be tested on different interfaces metal/ corrosive solution combinations. It is well known that pyrazole [3-6], bipyrazole[7-12], tripyrazole[13], triazole[14-20] and tetrazole [21-24] derivative compounds are excellent inhibitors of corrosion for many metals and alloys in aggressive media.

In the present work, we aim to study the effect of *N,N'*-bis[(3,5-dimethyl-1H-pyrazol-1-yl)methyl]piperazine (P2) and *N,N'*-bis[(3-ethylcarboxylate-5-methyl-1H-pyrazol-1-yl)methyl]piperazine (P3) on the corrosion of steel in 1M HCl. The behaviour of steel in 1M HCl with and without inhibitor is studied using gravimetric, potentiodynamic measurements and EIS. The effect of P2 and P3 is compared to that of piperazine (P1) molecule.

2. EXPERIMENTAL DETAILS

2.1. Chemistry

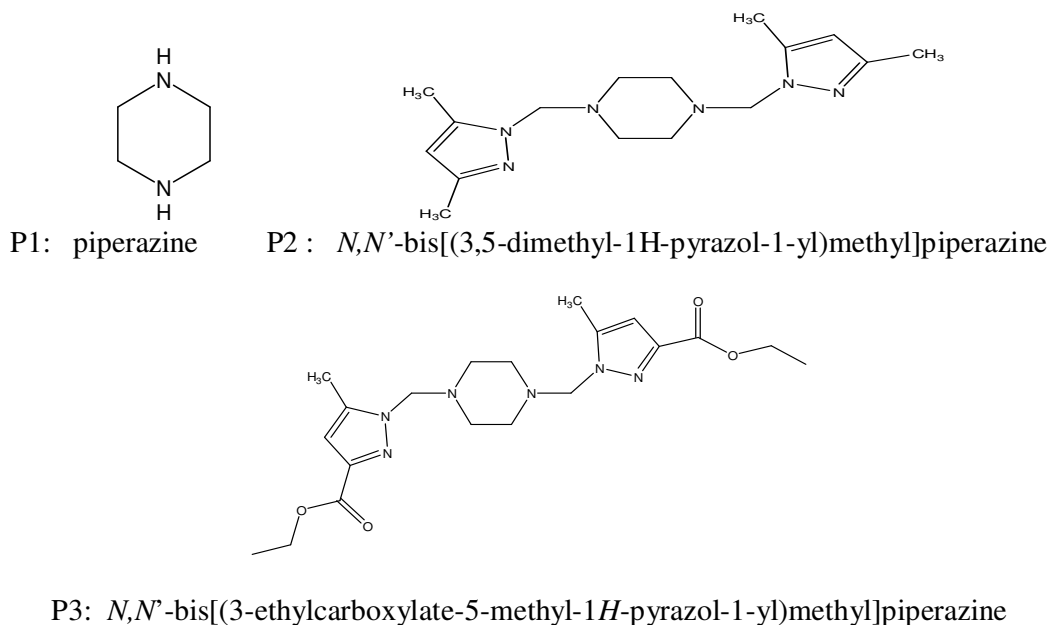


Figure 1. Synthesis of new *N,N'*-bipyrazole piperazine derivatives

2.2. Material preparation

The target bipyrazoles compounds (P2) [25-26] and (P3) [26] were prepared by condensation of two equivalents of hydroxymethylpyrazole with one equivalent of piperazine under gentle

conditions (room temperature, atmospheric pressure, 4-5 days), using anhydrous acetonitrile as solvent. The reaction is very slow but selective at room temperature.

N,N'-bis[(3,5-dimethyl-1*H*-pyrazol-1-yl)methyl]piperazine (P2). White powder, Yield 95%. Mp 158-160 °C (diethyl ether). IR (KBr, cm^{-1}): 2880 ($\nu_{\text{C-H}}$), 2800 ($\nu_{\text{C-H}}$), 1440 ($\nu_{\text{C=C}}$), 1140 ($\nu_{\text{C-N}}$). ^1H RMN (300MHz, CDCl_3) δ ppm: 2.20 (s, 6H, pyrazol- CH_3), 2.30 (s, 6H, pyrazol- CH_3), 2.60 (s, 8H, $\text{CH}_2\text{-CH}_2$), 4.60 (s, 4H, $\text{N-CH}_2\text{-N}$), 5.75 (s, 2H, pyrazol, CH). ^{13}C RMN (75 MHz, CDCl_3) δ ppm: 12 (pyrazol- CH_3), 14 (pyrazol- CH_3), 50($\text{N-CH}_2\text{-N}$), 106 (pyrazol, CH), 140 (pyrazol, C=C-CH_3), 146 (C=N). Anal. Calcd. for $\text{C}_{16}\text{H}_{26}\text{N}_6$: C 63.54, H 8.67, N 27.79, Found: C 63.64, H 8.75, N 27.81; m/z (M^+): 302.4

N,N'-bis[(3-ethylcarboxylate-5-methyl-1*H*-pyrazol-1-yl)methyl]piperazine (P3). White powder, Yield 92%. Mp 162-163 °C (diethyl ether). IR (KBr, cm^{-1}): 2880 ($\nu_{\text{C-H}}$), 2800 ($\nu_{\text{C-H}}$), 1720 ($\nu_{\text{C=O}}$), 1440 ($\nu_{\text{C=C}}$), 1140 ($\nu_{\text{C-N}}$). ^1H RMN (300MHz, CDCl_3) δ ppm: 1.45 (t, 6H, $-\text{O-CH}_2\text{-CH}_3$, $J = 6,9$ Hz), 2.20 (s, 8H, $\text{CH}_2\text{-CH}_2$), 2.40 (s, 6H, pyrazol- CH_3), 4.40 (q, 4H, $-\text{O-CH}_2\text{-CH}_3$, $J = 6,9$ Hz), 4.80 (s, 4H, $\text{N-CH}_2\text{-N}$), 6.60 (s, 2H, pyrazol, CH). ^{13}C RMN (75 MHz, CDCl_3) δ ppm: 12 (pyrazol- CH_3), 15 ($-\text{O-CH}_2\text{-CH}_3$), 50 ($-\text{CH}_2\text{-CH}_2-$), 61 ($\text{N-CH}_2\text{-N}$), 62 ($-\text{O-CH}_2\text{-CH}_3$), 109 (pyrazol, CH), 141 (pyrazol, C=C-CH_3), 143 (C=N), 163 (C=O). Anal. Calcd. for $\text{C}_{20}\text{H}_{30}\text{N}_6\text{O}_4$: C 57.40, H 7.23, N 20.08, Found: C 57.51, H 7.31, N 20.14; m/z (M^+): 418.5

Corrosion tests have been carried out on electrodes cut from sheets of mild steel. Steel containing 0.09% P, 0.38% Si, 0.01% Al, 0.05% Mn, 0.21% C, 0.05% S and the remainder iron were used for the measurement of weight loss and electrochemical studies. The surface preparation of the specimens was carried out using emery paper nos.260, 400 and 1200; they were degreased with AR grade ethanol, acetone and dried at room temperature before use. The solutions (1M HCl) were prepared by dilution of an analytical reagent grade 37% HCl with doubly distilled water. The solubility of the tested some sulphuric compounds are about 10^{-3} M in 1M HCl.

2.3. Gravimetric measurements

For weight loss measurements, each run was carried out in a double walled glass cell equipped with a thermostat-cooling condenser containing 100 ml test solution. The steel specimens used had a rectangular form ($1.5 \times 1.5 \times 0.05$ cm), was completely immersed at inclined position in the vessel. The immersion time for the weight loss was 6h at 308K. After 6 h of immersion, the electrode was withdrawn, rinsed with doubly distilled water, washed with ethanol, dried and weighed. Duplicate experiments were performed in each case and the mean value of the weight loss has been reported. The weight loss was used to calculate the corrosion rate (W) in milligrams per square centimetre per hour ($\text{mg}/\text{cm}^2 \text{ h}$).

2.4. Polarisation measurements

Electrochemical measurements were carried out in conventional three- electrode cylindrical Pyrex glass cell. The working electrode was a disc cut from iron (99.5% purity) sheet. The exposed

area to the corrosive solution was 1 cm^2 . A platine electrode and saturated calomel electrode (SCE) were used, respectively, as auxiliary and reference electrodes. All potentials are given in the SCE scale. The cell was thermostated at 308K.

The polarisation curves were recorded with a potentiostat type AMEL 550 using a linear sweep generator type AMEL 567 at scan rate of 30mV/min. Before recording the cathodic potentiokinetic curves up the corrosion potential, the iron electrode was polarised at 800 mV/SCE for 10min.

However, for anodic polarisation curves, the potential of the working electrode was swept from its open circuit potential value after 30 min at rest. Solutions were de-aerated with nitrogen. The nitrogen bubbling was maintained in the solutions during the electrode chemical measurements.

2.5. Electrochemical impedance spectroscopy (EIS)

The electrochemical impedance spectroscopy (EIS) measurements were carried out with the electrochemical system (Tacussel) which included a digital potentiostat model Voltalab PGZ 100 computer at E_{corr} after immersion in solution without bubbling, the circular surface of steel exposing of 1 cm^2 to the solution were used as working electrode. After the determination of steady-state current at a given potential, sine wave voltage (10 mV) peak to peak, at frequencies between 100 kHz and 10 MHz were superimposed on the rest potential. Computer programs automatically controlled the measurements performed at rest potentials after 30 min of exposure. The impedance diagrams are given in the Nyquist representation.

3. RESULTS AND DISCUSSION

3.1 Weight loss measurements

Table 1 resumes the corrosion rate obtained in 1 M HCl (W_{corr}^0) and at various contents of P2 and P3 (W_{corr}) determined at 308 K after 1 h of immersion rate and inhibition efficiencies E_w , determined by the relation:

$$E\% = \left[\frac{W_{\text{corr}} - W_{\text{corr}^{\text{inh}}}}{W_{\text{corr}}} \right] \times 100 \quad (1)$$

where W_{corr} and W_{corr}^0 are the corrosion rates of steel with and without bipyrazole derivatives.

It is clear that the addition of compounds reduces the corrosion rate in HCl solution. The inhibitory effect increases with the increase of bipyrazoles derivatives concentration. $E\%$ reaches a maximum of 92% at 10^{-3} M for P3. The effectiveness of P3 is due to the presence of the ester group which has misomer effect compared to inductif effect by methyl in P2. The protective properties of these compounds are probably due to the interaction between π -electrons of the pyrazole rings and heteroatom with positively charged steel surface [27-28]. We may conclude that compounds (P2 and P3) are good inhibitors of steel corrosion in 1 M HCl solution.

Table 1. Gravimetric results of steel in 1 M HCl with and without addition of the bipyrazole derivatives at various concentrations.

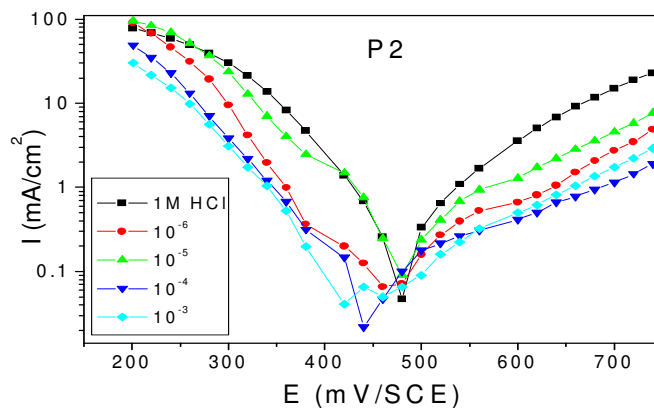
Inhibitors	Concentration(M)	W(mg/cm ² .h)	E _w (%)	Θ
Blanc	1	1.855	-	-
P1	10 ⁻³	1.360	26.00	0.2600
P2	10 ⁻³	0.1652	91.1	0.9110
	5×10 ⁻⁴	0.1771	90.45	0.9045
	10 ⁻⁴	0.4075	78.00	0.7800
	5×10 ⁻⁵	0.7026	62.13	0.6213
	10 ⁻⁵	0.8244	55.55	0.5555
	10 ⁻⁶	1.274	31.30	0.3130
P3	10 ⁻³	0.1375	92.50	0.9250
	5×10 ⁻⁴	0.1703	91.00	0.9100
	10 ⁻⁴	0.2445	86.81	0.8681
	5×10 ⁻⁵	0.3050	83.56	0.8356
	10 ⁻⁵	0.3001	83.80	0.8380
	10 ⁻⁶	0.3024	83.00	0.8300

3.2 Electrochemical polarisation measurements

In the case of polarisation method the relation determines the inhibition efficiency (E%):

$$E_i = 100 \times \left(1 - \frac{I_{corr}}{I_{corr}^{\circ}} \right) \tag{2}$$

where I^o_{corr} and I_{corr} are the uninhibited and inhibited corrosion current densities, respectively, determined by extrapolation of cathodic Tafel lines to corrosion potential. Polarisation behaviour of steel in 1 M HCl in the presence and absence of inhibitors is shown in Fig. 2. The values of corrosion current (I_{corr}), corrosion potential (E_{corr}), cathodic Tafel slope (β_c) and inhibition efficiency (E%), are collected in Table 2.



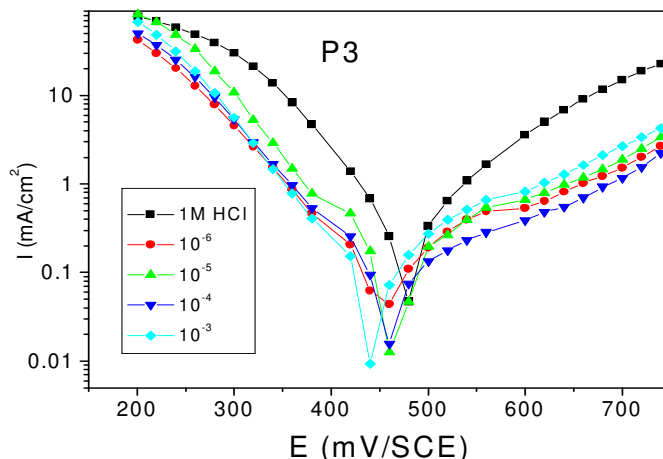


Figure 2. Typical polarisation curves of steel in 1 M HCl for various concentrations of P2 and P3.

The examination of Fig. 2 and Table 2 shows that the addition of P2 and P3 decreases current density. The decrease is more pronounced with the increase of the inhibitor concentration. The Tafel plots indicate that the mechanism of hydrogen reduction is activation control. The presence of pyrazoles does not affect the cathodic Tafel slope, indicating that the mechanism of H^+ reduction is not modified with the P2 and P3 concentration. Also, the corrosion potential is almost constant in the presence of the inhibitors. Corrosion potential E_{corr} shifts have no definite trend which indicates that these molecules act as mixed type inhibitors by simple blocking the available surface area. The inhibitor molecules decrease the surface area of corrosion and only cause inactivation of a part of the surface with respect to the corrosion medium. The inhibition efficiency reaches 86% and 89 % at 10^{-3} M of P2 and P3, respectively. This phenomenon is interpreted by the adsorption of the molecules on steel surface leading to the increase of the surface coverage θ defined by $E\% / 100$. $E\%$ increases with compound concentration. We may conclude that P2 and P3 are effective inhibitors of steel corrosion in molar HCl.

Table 2. Polarisation parameters for steel in acid at different contents of P2 and P3 at 308 K.

Inhibiteurs	Concentration (M)	E_{corr} (mv/SCE)	I_{corr} (mA/cm ²)	β_c (mV/dec)	E_I (%)
HCl	1M	-478	0.5735	-152.0	-
P2	10^{-6}	-500.4	0.2456	-160.2	57.00
	10^{-5}	-485.6	0.1359	-168.4	76.30
	10^{-4}	-463.5	0.0935	-206.9	84.00
	10^{-3}	-463.2	0.0801	-195.1	86.03
P3	10^{-6}	-466.1	0.1270	-225.8	79.00
	10^{-5}	-488.0	0.0885	-132.2	84.60
	10^{-4}	-482.0	0.0847	-204.3	85.23
	10^{-3}	-476.2	0.0656	-108.3	89.00

3.3. Electrochemical impedance measurements

Fig.3 show Nyquist plots for mild steel in 1M HCl in absence and presence of different concentrations of bipyrazole compounds P2 and P3 in the concentration range 10^{-6} to 10^{-3} M at 308C. Nyquist plots consist of one capacitive loop with one time constant. The charge transfer resistance values (R_{ct}) are calculated from the difference in impedance at lower and higher frequencies, as described elsewhere [29]. To obtain the double layer capacitance (C_{dl}) the frequency at which the imaginary part of the impedance is maximum ($-Z_{img,max}$) is found and C_{dl} values are calculated from the following equation [30]:

$$C_{dl} = \frac{1}{\omega R_t} \quad \text{Where } \omega = 2\pi f_{max} \quad (3)$$

The interpretation of Nyquist Fig. 3 allow to determine the electrochemical parameters of the steel electrode and to acquire information about the corrosion process and mechanism. As in Table 3, the corrosion rate can be calculated by determining the reciprocal of the charge transfer resistance ($1/R_{ct}$). Data in Table3 shows that these compounds obviously inhibit the corrosion of mild steel in 1 M HCl. The inhibition efficiency increased by increasing the

concentration of the studied inhibitors. The inhibition efficiency is calculated using charge transfer resistance from equation [28]:

$$E(\%) = \frac{R_{t/inh} - R_t}{R_{t/inh}} \cdot 100 \quad (4)$$

where R_{ct} and R_{ct}^{inh} are the charge transfer resistance values in absence and presence of inhibitor for mild steel in 1 M HCl, respectively. By increasing the inhibitor concentration the R_{ct} values increase but C_{dl} values decrease. Characterization of the adsorption and desorption and film formation on the metal electrode surface may be studied by determining its capacitance C_{dl} . The decrease in the C_{dl} value is due to the adsorption of the inhibitors on the steel surface [31]. The adsorption of these inhibitors on mild steel surface can occur either directly on the basis of donor–acceptor interaction between the π electrons (of the double bonds) and the vacant d-orbitals of steel surface atoms or interaction of them with already adsorbed chloride ions as proposed [32-33]. Adsorption might also occur in the cationic form with positively charged part of the molecule oriented toward negatively charges metal surface. This fact supports the observed decrease in C_{dl} values in the EIS measurement at the corrosion potential, Table 3. It is clear that compound P3 is the best inhibitor, it contain the ester group with its powerful mesomer effect which facilitate the delocalization of electron. Fig.3 indicate that the impedance response of mild steel in uninhibited 1 M HCl has significantly changed after the addition of bipyrazole derivatives in the corrosive system. The results described above can be interpreted in terms of equivalent circuit of the electrical double layer shown in Fig. 4, which has been used previously to model the iron/acid interface [34]. Nyquist plots, Fig. 3, are

depressed into the Zr (real axis) and not perfect semi-circles as a result of the roughness and other in homogeneities of the metal surface [35]. This kind of phenomena is known as “the dispersing effect” [36]. Also, It can be explained as follows:

On the metal side, electrons control the charge distribution whereas on the solution side it is controlled by ions. Since ions are much larger than electrons, the equivalent ions to the charge on the metal will occupy quite large volume on the solution side of the double layer [34]. Decreasing the capacitance C_{dl} , in Table 3, which can result from a decrease in dielectric constant and/or an increase in the thickness of the electrical double layer, suggests that the inhibitor molecules act by adsorption at the steel/acid interface [37].

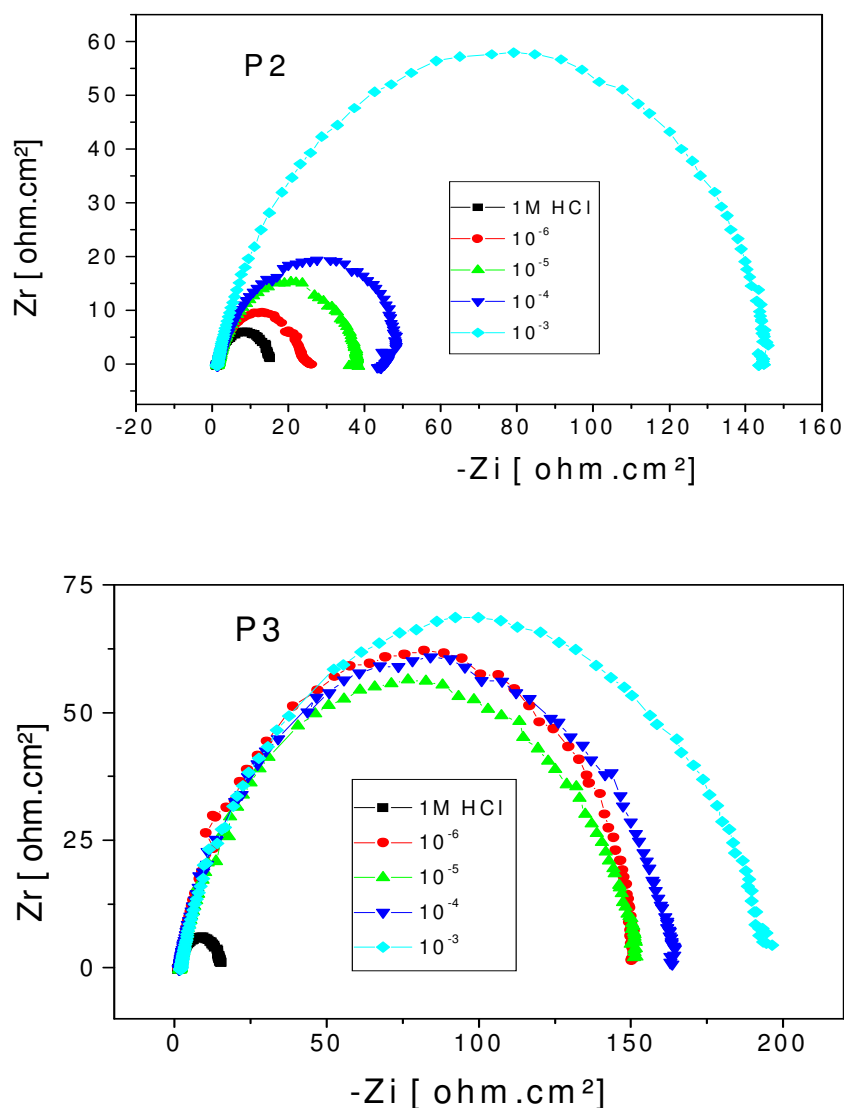
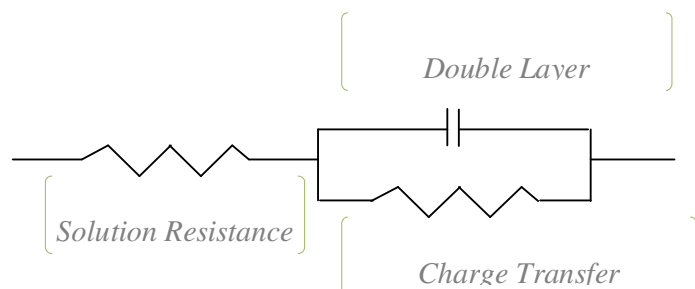


Figure 3. Nyquist diagrams for steel in 1M HCl with different concentrations of P2 and P3

Table 3. Impedance data of mild steel in 1 M HCl in absence and presence of different concentrations from bipyrzole acid derivatives

Inhibitor	concentration	$R_s / \Omega \text{ cm}^2$	$R_t / \Omega \text{ cm}^2$	F_{\max} / Hz	$C_{dl} / \mu\text{F cm}^2$	E / %
P2	1M HCl	2	20	113.7	70.00	-
	10^{-3}M	1.81	144	22.35	49.43	86.11
	10^{-4}M	1.82	48.57	63.41	51.67	48.15
	10^{-5}M	1.67	36.29	79.37	55.25	44.88
	10^{-6}M	1.61	23.23	111.76	61.30	13.90
P3	10^{-3}M	1.60	194.4	15.82	51.72	89.71
	10^{-4}M	1.68	151	17.88	58.92	86.75
	10^{-5}M	1.50	163	17.87	54.62	87.73
	10^{-6}M	1.93	150	20.08	52.83	86.66

**Figure 4.** Suggested equivalent circuit model for the studied system.

3.4. Effect of temperature

We have studied the temperature influence on the efficiency of P2 and P3. For this purpose, we made weight-loss measurements in the temperature range 318 - 348 K, in the presence and absence of the compound at various concentrations during 1 h of immersion. The corresponding data are shown in Table 4. It is clear that the increase of corrosion rate is more pronounced with the rise of temperature for blank solution. In the presence of the tested molecules, W_{corr} is highly reduced. Hence we note that the efficiency depends on the temperature and decreases with the rise of temperature from 318 to 348 K. This can be explained by the decrease of the strength of the adsorption process at elevated temperature and suggested a physical adsorption mode. To calculate activation thermodynamic parameters of the corrosion reaction such as the energy E_a , the entropy ΔS_a° and the enthalpy ΔH_a° of activation, Arrhenius Eq. (5) and its alternative formulation called transition state Eq. (6) were used:

$$W = k \exp\left(-\frac{E_a}{RT}\right) \quad (5)$$

$$W = \frac{RT}{Nh} \exp\left(\frac{\Delta S_a^\circ}{R}\right) \exp\left(-\frac{\Delta H_a^\circ}{RT}\right) \quad (6)$$

where T is the absolute temperature, K is a constant and R is the universal gas constant, h is Plank's constant, and N is Avogadro's number.

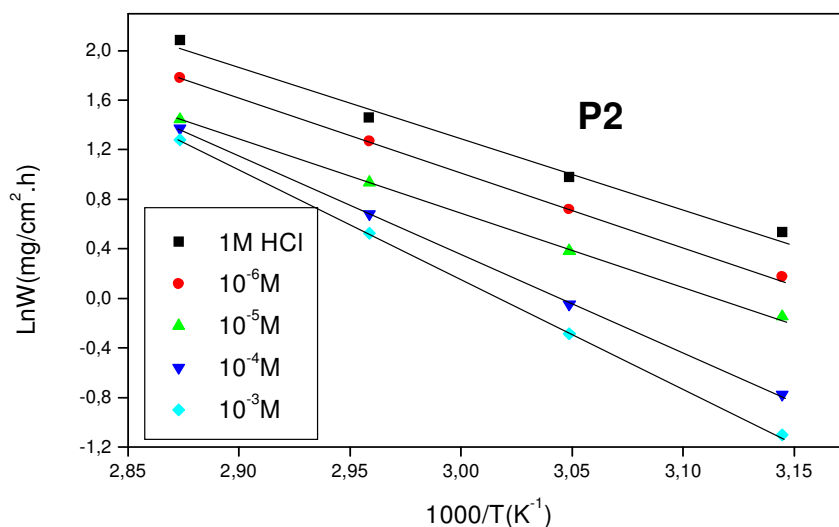
Table 4. Effect of temperature on the corrosion rate of steel in 1M HCl (W_0) without and with P2 and P3 at 10^{-3} to 10^{-6} M and the corresponding corrosion inhibition efficiency.

Inhibitor	Temperature (K)	Concentration (M)	W (mg/cm ² .h)	E %	θ
P2	318	blank 1M	1.908	-	
		10^{-3}	0.3820	80,00	0,8000
		10^{-4}	0.5440	71,50	0,7150
		10^{-5}	0.9671	49,31	0,4931
		10^{-6}	1.370	28,07	0,2807
	328	blank 1M	2.092	-	
		10^{-3}	0.6250	70,12	0,7012
		10^{-4}	0.7928	62,10	0,6210
		10^{-5}	1.204	42,41	0,4241
		10^{-6}	1.665	20,37	0,2037
	338	blank 1M	3.890	-	
		10^{-3}	1.510	61,17	0,6117
		10^{-4}	1.741	55,23	0,5523
		10^{-5}	2.549	34,47	0,3447
		10^{-6}	3.227	17,04	0,1704
	348	blank 1M	8.744	-	
		10^{-3}	4.143	52,61	0,5261
		10^{-4}	4.615	47,21	0,4721
		10^{-5}	6.850	21,67	0,3447
		10^{-6}	-	-	-

Inhibitor	Temperature (K)	Concentration (M)	W (mg/cm ² .h)	E %	θ
P3	318	blank 1M	1.908	-	
		10^{-3}	0.243	87,26	0,8726
		10^{-4}	0.4357	77,16	0,7716
		10^{-5}	0.9200	62,00	0,6200
		10^{-6}	1.360	45,00	0,4500
	328	blank 1M	2.092	-	
		10^{-3}	0.3974	81,00	0,8100
		10^{-4}	0.6453	69,15	0,6915
		10^{-5}	0.7171	65,72	0,6572

		10^{-6}	0.7671	63,33	0,6333
338	blank 1M		3.890	-	
	10^{-3}		1.244	68,00	0,6800
	10^{-4}		1.668	57,10	0,5710
	10^{-5}		1.980	49,11	0,4911
	10^{-6}		2.283	41,31	0,4131
348	blank 1M		8.744	-	
	10^{-3}		2.971	66,02	0,6602
	10^{-4}		4.388	49,81	0,4981
	10^{-5}		5.231	40,17	0,4017
	10^{-6}		6.100	30,23	0,3023

The activation energy E_a is calculated from the slope of the plots of $\ln(W_{\text{corr}})$ vs. $1/T$ (Fig. 5). Plots of $\ln(W_{\text{corr}}/T)$ vs. $1/T$ give a straight line with a slope of $\Delta H^\circ/R$ and an intercept of $(\text{Log}(R/Nh) + \Delta S^\circ/R)$, as shown in Fig. 6. From this relation the values of ΔH° and ΔS° can be calculated (Table 5). The decrease of P2 and P3 efficiencies with temperature rise leads to a higher value of E_a , when compared to that in an uninhibited acid, and it is interpreted as an indication of an electrostatic character of the inhibitor's adsorption [38]. But, E_a variation is not the unique parameter to affirm of such mode of adsorption. Other ones can be considered, such as free adsorption enthalpy ΔG_{ads}^0 and enthalpy ΔH_{ads}^0 , which will be discussed in next paragraph. The positive values of ΔH° mean that the dissolution reaction is an exothermic process and that the dissolution of steel is difficult [39]. Practically E_a and ΔH° are of the same order. Also, the entropy ΔS° increases more positively with the presence of the inhibitor than in the presence of the non-inhibited one. This reflects the formation of an ordered stable layer of the inhibitor on the steel surface [40]. From the previous data, we can conclude that P2 and P3 is an effective inhibitor.



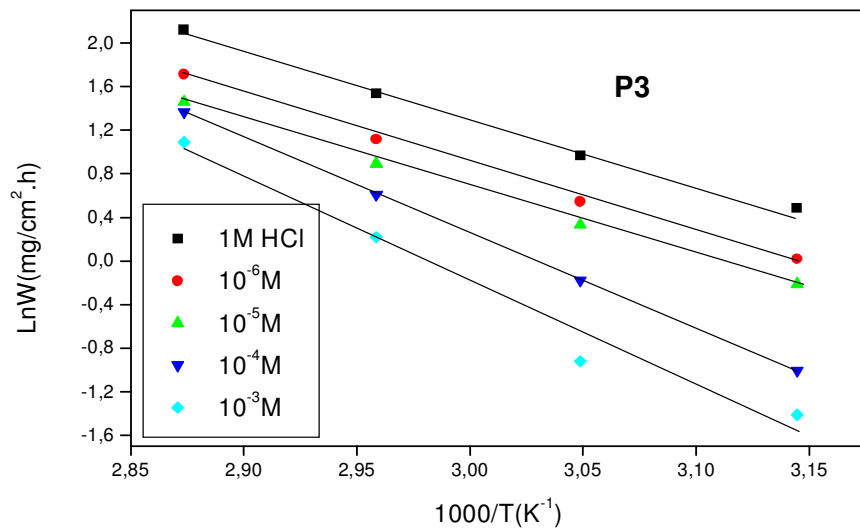


Figure 5. Arrhenius plots for steel in 1M HCl in the absence and presence of P2 and P3

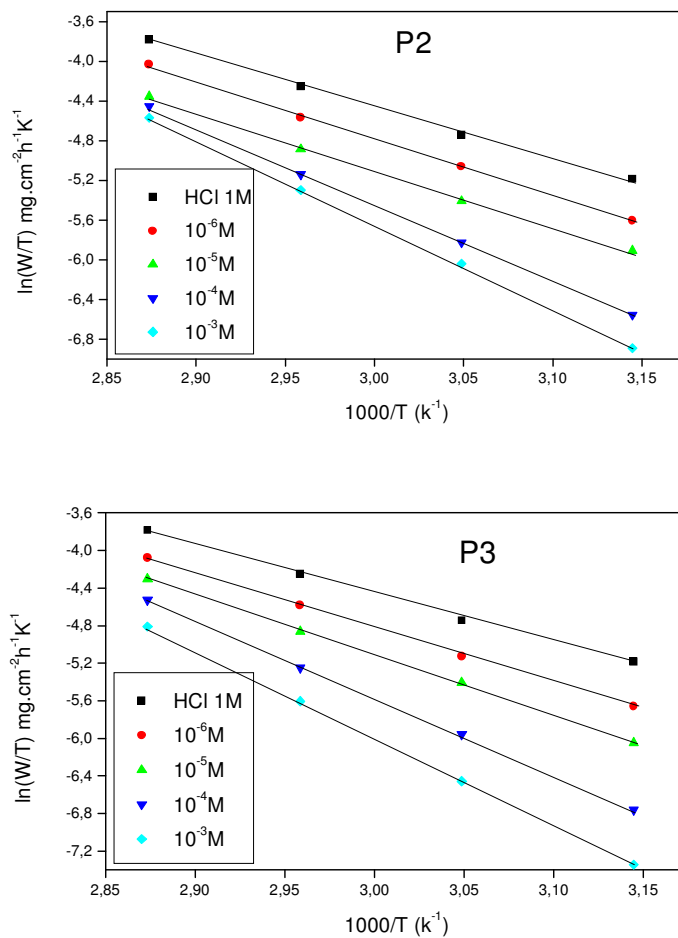


Figure 6. The relation between log (W / T) vs. 1 / T for steel at different concentrations of P2 and P3.

Table 5. The values of activation parameters E_a , ΔH_a^0 and ΔS_a^0 for mild steel in 1M HCl in the absence and the presence of different concentrations of P2 and P3.

	Concentration (M)	E_a (kJ mol ⁻¹)	ΔH_a^0 (kJ mol ⁻¹)	ΔS_a^0 (J mol ⁻¹ K ⁻¹)	$E_a - \Delta H_a^0$ (kJ mol ⁻¹)
Blank	Blank	47.33	44.54	-101.87	2.79
P2	10 ⁻⁶ M	50.23	47.40	-95.35	2.83
	10 ⁻⁵ M	49.83	46.95	-99.40	2.88
	10 ⁻⁴ M	65.93	63.08	-53.80	2.85
	10 ⁻³ M	73.63	70.90	-32.03	2.73
P3	10 ⁻⁶ M	50.59	47.89	-96.46	2.70
	10 ⁻⁵ M	56.64	54.08	-79.38	2.56
	10 ⁻⁴ M	72.18	69.42	-35.80	2.76
	10 ⁻³ M	79.40	80.09	-17.74	-

3.5 Adsorption isotherm

Basic information on the interaction between the inhibitor and the carbon steel can be provided by the adsorption isotherm. Two main types of interaction can describe the adsorption of the organic compounds: physical adsorption and chemisorption. These are influenced by the chemical structure of the inhibitor, the type of the electrolyte and the charge and nature of the metal. The surface coverage θ of the metal surface by the adsorbed inhibitor was calculated [41] assuming no change in mechanism of the cathodic reaction using the equation:

$$\theta = \frac{W_{corr} - W_{corr(inh)}}{W_{corr}} \quad (7)$$

Where W_{corr} and $W_{corr(inh)}$ are the corrosion rates in the presence and absence of the inhibitor.

The θ values for different inhibitor concentrations at 35 to 80 °C were tested by fitting to various isotherms. By far the best fit was obtained with the Langmiur isotherm. According to this isotherm θ is related to concentration inhibitor C via

$$\frac{C}{\theta} = \frac{1}{K} + C \quad (8)$$

$$\text{With } K = \frac{1}{55.5} \exp\left(\frac{-\Delta G_{ads}^0}{RT}\right) \quad (9)$$

Where K is the adsorptive equilibrium constant and ΔG_{ads}^0 is the free energy of adsorption.

It was found that Fig.7 (plot of θ/C versus C) gives straight lines with slope equal or nearly equal to 1.00 for 45, 55, 65 and 75°C. This result indicates that the adsorption of compound under consideration on steel/acidic solution interface at all temperatures follows the Langmuir adsorption isotherm.

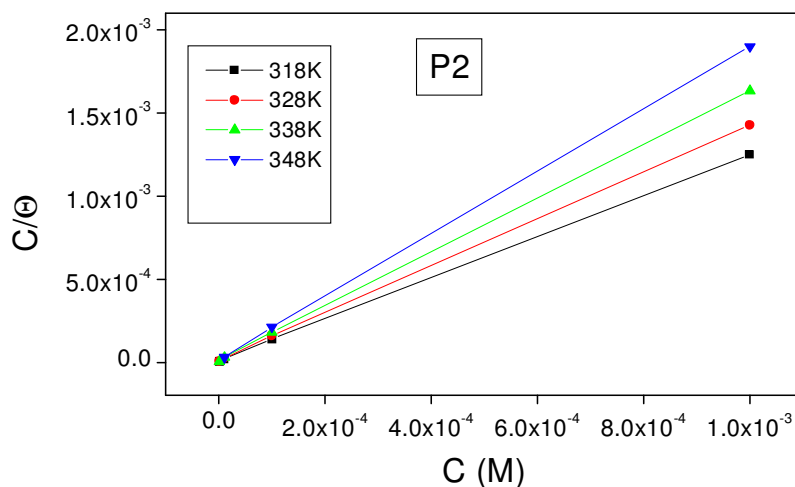
Thermodynamic parameters are important to study the inhibitive mechanism. The values of $\Delta G_{\text{ads}}^{\circ}$ at different temperatures were estimated from the values of K and Eq. (9). The negative values of $\Delta G_{\text{ads}}^{\circ}$ show that the adsorption of organic compounds studied is a spontaneous process [42-45] under the experimental conditions described. It is well known that values of $-\Delta G_{\text{ads}}^{\circ}$ of the order of 20 kJ mol^{-1} or lower indicate a physisorption, those of order of 40 kJ mol^{-1} or higher involve charge sharing or a transfer from the inhibitor molecules to the metal surface to form a coordinate type of bond [46-47]. On the other hand, Metikoš-Huković et al. [48] describe the interaction between thiourea and iron ($\Delta G_{\text{ads}}^{\circ} = -39 \text{ kJ mol}^{-1}$) as chemisorption. The same conclusion was given by Wang et al. concerning the interaction between mercapto-triazole and mild steel ($\Delta G_{\text{ads}}^{\circ} = -32 \text{ kJ mol}^{-1}$) [49].

Moreover, Bayoumi and Ghanem consider that the adsorption of naphthalene disulphonic acid on the mild steel was principally by chemisorption ($\Delta G_{\text{ads}}^{\circ} = -28.47 \text{ kJ mol}^{-1}$) [50]. Thus, the $\Delta G_{\text{ads}}^{\circ}$ value obtained here shows that in the presence of 1M HCl, chemisorption of inhibitor on the carbon steel may occur.

Considering the values of enthalpy and entropy of the inhibition process have no distinct changes in the temperature range studied, the thermodynamic parameters $\Delta H_{\text{ads}}^{\circ}$ and $\Delta S_{\text{ads}}^{\circ}$ for the adsorption of P2 and P3 on carbon steel can be calculated from the following equation:

$$\Delta G_{\text{ads}}^{\circ} = \Delta H_{\text{ads}}^{\circ} - T\Delta S_{\text{ads}}^{\circ} \quad (10)$$

where $\Delta H_{\text{ads}}^{\circ}$ and $\Delta S_{\text{ads}}^{\circ}$ are the variation of enthalpy and entropy of the adsorption process, respectively. The values of $\Delta G_{\text{ads}}^{\circ}$ were plotted against T . This plot is shown in Fig.8. It should be noted that the entropy change of adsorption $-\Delta S_{\text{ads}}^{\circ}$ is the slope of the straight line $\Delta G_{\text{ads}}^{\circ}$ vs T according to Eq. (10). The intercept of the straight line is used to calculate the heat of adsorption $\Delta H_{\text{ads}}^{\circ}$. The calculated values are depicted in Table 6. The negative sign of $\Delta H_{\text{ads}}^{\circ}$ indicates that the adsorption of inhibitor molecules is an exothermic process. $\Delta S_{\text{ads}}^{\circ}$ in the presence of inhibitor is large and positive meaning that an increase in disordering takes places in going from reactants to the metal adsorbed species reaction complex [51].



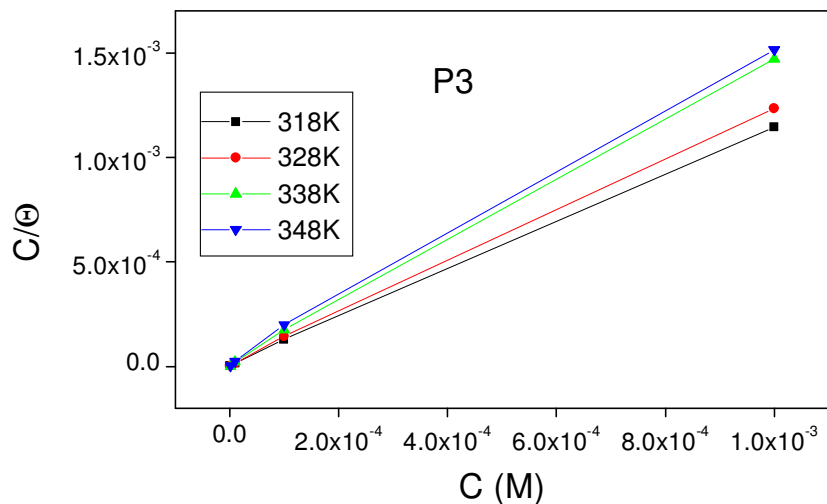


Figure 7. Langmuir adsorption plots for carbon steel in 1M HCl containing different concentrations of inhibitor at different temperatures.

Table 6. The thermodynamic parameters for some inhibitors studied at carbon steel surface in 1M HCl

Inhibitor	Temperature (K)	A	K	B	ΔG°_{ads} (kJ mol ⁻¹)	ΔH°_{ads} (kJ mol ⁻¹)	ΔS°_{ads} (J mol ⁻¹ K ⁻¹)
P2	318	8.36.10 ⁻⁶	119617.22	1,02	-41.56	-18.95	71.10
	328	1.04.10 ⁻⁵	96153.84	1,04	-42.27		71.09
	338	1.16.10 ⁻⁵	86206.89	1,06	-43.25		71.89
	348	1.64.10 ⁻⁵	60975.61	1,08	-43.53		70.63
P3	318	6.85.10 ⁻⁶	145985.4	1,01	-42.08	-32.22	31.00
	328	7.92.10 ⁻⁶	126262.62	1,02	-43.02		32.92
	338	1.15.10 ⁻⁵	86956.52	1,04	-43.27		32.69
	348	1.96.10 ⁻⁵	51020.41	1,05	-43.01		31.00

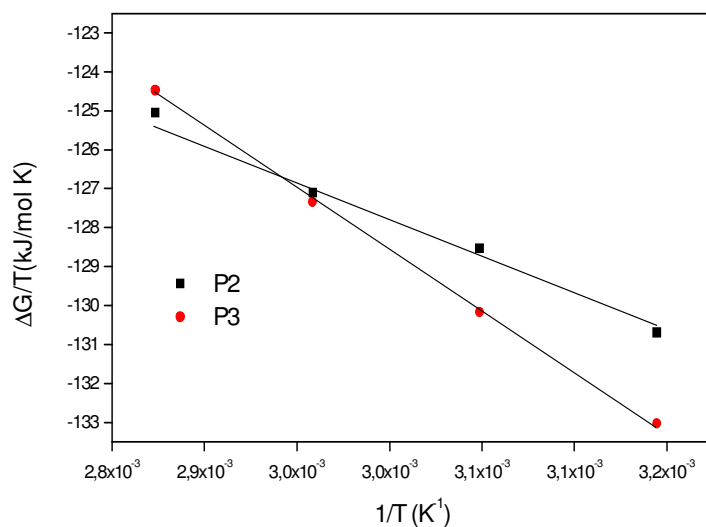


Figure 8. The relationship between ΔG°_{ads} and T

Moreover so since adsorption enthalpy is small and negative and adsorption entropy is large and positive value, it can be deduced that the driving force for the adsorption of adsorbate is the increase in entropy during the process of adsorption rather than the decrease in enthalpy.

On the other hand, ΔH°_{ads} can be also calculated according to the Van't Hoff equation:

$$\ln K = \frac{-\Delta H^{\circ}_{ads}}{RT} + \text{const} \tag{11}$$

Fig.9. shows the plot of $\ln K$ versus $1/T$ which gives straight lines with slopes of $\frac{\Delta H^{\circ}_{ads}}{R}$ and intercept of $\frac{\Delta S^{\circ}_{ads}}{R} - \ln 55.5$. The calculated ΔH°_{ads} using the Van't Hoff equation confirming the exothermic behaviour of the adsorption of inhibitors on the steel surface. Values of ΔH°_{ads} obtained by the both method are in good agreement (table 7). Moreover, the deduced ΔS°_{ads} value is very close to that given in Table.6

Table 7. van't Hoff, Gibbs–Helmholtz, and thermodynamic parameters

Equation of	ΔH°_{ads} (kJ mol ⁻¹) van't Hoff	ΔH°_{ads} (kJ mol ⁻¹) Gibbs–Helmholtz
P2	-19.50	-18.95
P3	-32.45	-32.22

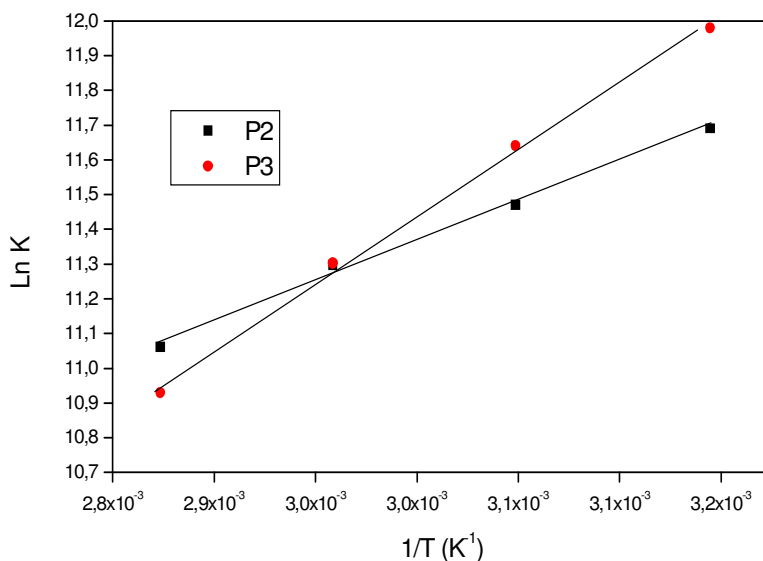


Figure 9. The relationship between $\ln K$ and $1/T$.

In the present study, chemisorption is evident from, the apparent activation energy of the corrosion that is lower in presence of inhibitors than in its absence, the inhibition efficiency, which is temperature independent and the large negative values of $\Delta G^{\circ}_{\text{ads}}$. Therefore, organic compounds may adsorb on a metal surface in the form of a neutral molecule via the chemisorption mechanism [52] involving the sharing of electrons between the nitrogen atoms and iron. The covalent bond with the metal is most probably formed between the unpaired electrons of the N-atom.

4. CONCLUSIONS

The following results can be drawn from this study:

1. bipyrazole derivatives are very good inhibitors and acts as mixed type inhibitors for mild steel in hydrochloric acid solution. Corrosion inhibition efficiencies are in the order $P3 > P2 > P1$.
2. Inhibition efficiencies increases by increasing the inhibitor concentration and inhibition occur through adsorption of the inhibitor on the mild steel surface. The adsorption of these inhibitors obeys the Langmuir adsorption isotherm.
3. Double layer capacitances decreases with respect to the blank solution when these inhibitors are added. This fact may be explained on the basis of adsorption of these inhibitors on the steel surface.
4. In determining the corrosion, the electrochemical studies and weight loss measurements gave similar results.

References

1. A. Popova, E. Sokolova, S. Raicheva, M. Christov, *Corros. Sci.* 45 (2003) 33
2. E.A. Noor, *Corros. Sci.* 47 (2005) 33
3. A. Aouniti, B. Hammouti, M. Brighli, S. Kertit, F. Berhili, S. ElKadiri, A. Ramdani, *J. Chim. Phys.* 93 (1996) 1262.
4. M. Abdallah, M.M. El Naggar, *Mater. Chem. Phys.* 71 (2001) 291.
5. A.G. Gad Allah, H.M. Tamous, *J. Appl. Electrochem.* 20 (1990) 488.
6. A.G. Gad Allah, H. Moustafa, *J. Appl. Electrochem.* 22 (1992) 644.
7. K. Tebbji, H. Oudda, B. Hammouti, M. Benkaddour, M. ElKodadi, F. Malek, A. Ramdani, *Appl. Surf. Sci.* 241 (2005) 326.
8. F. Touhami, A. Aouniti, S. Kertit, Y. Abed, B. Hammouti, A. Ramdani, K. El Kacemi, *Corros. Sci.* 42 (2000) 929.
9. A. Dafali, B. Hammouti, R. Touzani, S. Kertit, A. Ramdani, K. ElKacemi, *Anti-Corros. Methods Mater.* 49 (2002) 96.
10. F. Touhami, B. Hammouti, A. Aouniti, S. Kertit, *Ann. Chim. Sci. Mater.* 24 (1999) 581.
11. A. El-Ouafi, B. Hammouti, H. Oudda, S. Kertit, R. Touzani, A. Ramdani, *Anti-Corros. Methods Mater.* 49 (2002) 199.
12. K. Tebbji, H. Oudda, B. Hammouti, M. Benkaddour, M. El Kodadi, A. Ramdani, *Colloids Surf., A Physicochem. Eng. Asp.* 259 (2005) 157.
13. M. Elayyachy, M. El Kodadi, B. Hammouti, A. Ramdani, A. El Idrissi, *Pigm. Resin Technol.* 33 (2004) 375.

14. F. Bentiss, M. Traisnel, L. Gengembre, M. Lagrenée, *Appl. Surf. Sci.* 161 (2000) 194.
15. S. Ramesh, S. Rajeswari, S. Maruthamuthu, *Appl. Surf. Sci.* 229(2004)214
16. A.B. Tadros, B.A. Abdenaby, *J. Electroanal. Chem.* 246 (1988) 433.
17. R. Agrawal, T.K.G. Namboodhiri, *J. Appl. Electrochem.* 22 (1992) 383.
18. G. Xue, J. Ding, P. Lu, J. Dong, *J. Phys. Chem.* 95 (1991) 7380.
19. H.L. Wang, H.B. Fan, J.S. Zheng, *Mater. Chem. Phys.* 77 (2002) 655.
20. M.A. Quraishi, D. Jamal, *Mater. Chem. Phys.* 68 (2001) 283.
21. S. Kertit, B. Hammouti, *Appl. Surf. Sci.* 93 (1996) 5966.
22. S. Kertit, H. Essouffi, B. Hammouti, M. Benkaddour, *J. Chim. Phys.* 95 (1998) 2072.
23. S. Kertit, K. Bekkouche, B. Hammouti, *Rev. Metal.* 95 (1998) 251-.
24. F. Chaouket, B. Hammouti, S. Kertit, K. ElKacemi, *Bull. Electrochem.* 17 (2001) 311.
25. A. Elfatmi, M. Daoudi, N. Belarbi, A. Kerbal, M.F. Baba, B. Elbali, M. Bolte, M. Mchich, T. Benhadda, *Molbank* (2006) M467.
26. S. Radi, Y. Toubi, A. Hakkou, F. Souana, I. Himri, M. Bouakka, *Let. Drug Des. Discov.* 9 (2012) in press
27. M. Bouklah, A. Attayibat, B. Hammouti, A. Ramdani, S. Radi, M. Benkaddour. *Appl. Sur. Sci.* 242 (2005) 399
28. K. Tebbji, I. Bouabdellah, A. Aouniti, B. Hammouti, H. Oudda, M. Benkaddour, A. Ramdani. *Mat. Let.* 61 (2007) 799
29. S.S. Abdel-Rehim, Magdy A.M. Ibrahim, K.F. Khaled, *J. Appl. Electrochem.* 29 (1999) 593.
30. M. Bouklah, A. Ouassini, B. Hammouti, A. El Idrissi. *Appl. Sur. Sci.* 250 (2005) 50
31. I.L. Rosenfeld, *Corrosion Inhibitors*, McGraw-Hill, New York, 1981.
32. T. Murakawa, S. Nagaura, N. Hackerman, *Corros. Sci.* 7 (1967) 79.
33. N. Hackerman, E.S. Snavely, J.S. Payne, *J. Electrochem. Soc.* 113 (1966) 677.
34. H. Ashassi-Sorkhabi, B. Shaabani, D. Seifzadeh, *Electrochim. Acta* 50 (2005) 3446.
35. K.F. Khaled, *Appl. Surf. Sci.* 230 (2004) 307.
36. K.F. Khaled, *Appl. Surf. Sci.* 252 (2006) 4120.
37. E. McCafferty, N. Hackerman, *J. Electrochem. Soc.* 119 (1972) 146.
38. A. Popova, *Corros. Sci.* 49 (2007) 2144.
39. N.M. Guan, L. Xueming, L. Fei, *Mater. Chem. Phys.* 86 (2004) 59.
40. A. Yurt, A. Balaban, S.U. Kandemir, G. Bereket, B. Erk, *Mater. Chem. Phys.* 85 (2004) 420.
41. T. Tsuru, S. Haruyama, B. Gijutsu, *J. Jpn. Soc. Corros. Eng.* 27, (1978) 573
42. A.E. Fouda, H.A. Mostafa, H.M. Abu-Elnader, *Monatshefte für Chem.* 104, (1989) 501
43. M. Bouklah, N. Benchat, B. Hammouti, A. Aouniti, S. Kertit, *Mater. Lett.* 60, 1901 (2006)
44. M. Bouklah, B. Hammouti, M. Benkaddour, A. Attayibat, S. Radi, *Pigm. Resin Techn* 34, 197 (2005)
45. M. Bouklah, B. Hammouti, M. Benkaddour, T. Benhadda, *J. Appl. Electrochem* 35, (2005) 1095
46. F.M. Donahue, K. Nobe, *J. Electrochem. Soc.* 112, (1965) 886
47. E. Kamis, F. Belluci, R.M. Latanision, E.S.H. El-Ashry, *Corrosion.* 47, (1991) 677
48. M. Metikoš-Huković, R. Babić, Z. Grubać, *J. Appl. Electrochem.* 26, (1996) 443
49. H.-L. Wang, H.-B. Fan, J.-S. Zheng, *Mat. Chem. Phys.* 77, (2002) 655
50. F.M. Bayoumi, W.A. Ghanem, *Mater. Lett.* 59, 3(2005) 806
51. H.-L. Wang, H.-B. Fan, J.-S. Zheng, *Mat. Chem. Phys.* 77, (2002), 655
52. M.P. Soriaga, *Chem. Rev.* 90, (1990) 771